Soft Matter

Accepted Manuscript

ROYAL SOCIETY OF CHEMISTRY

www.rsc.org/softmatter

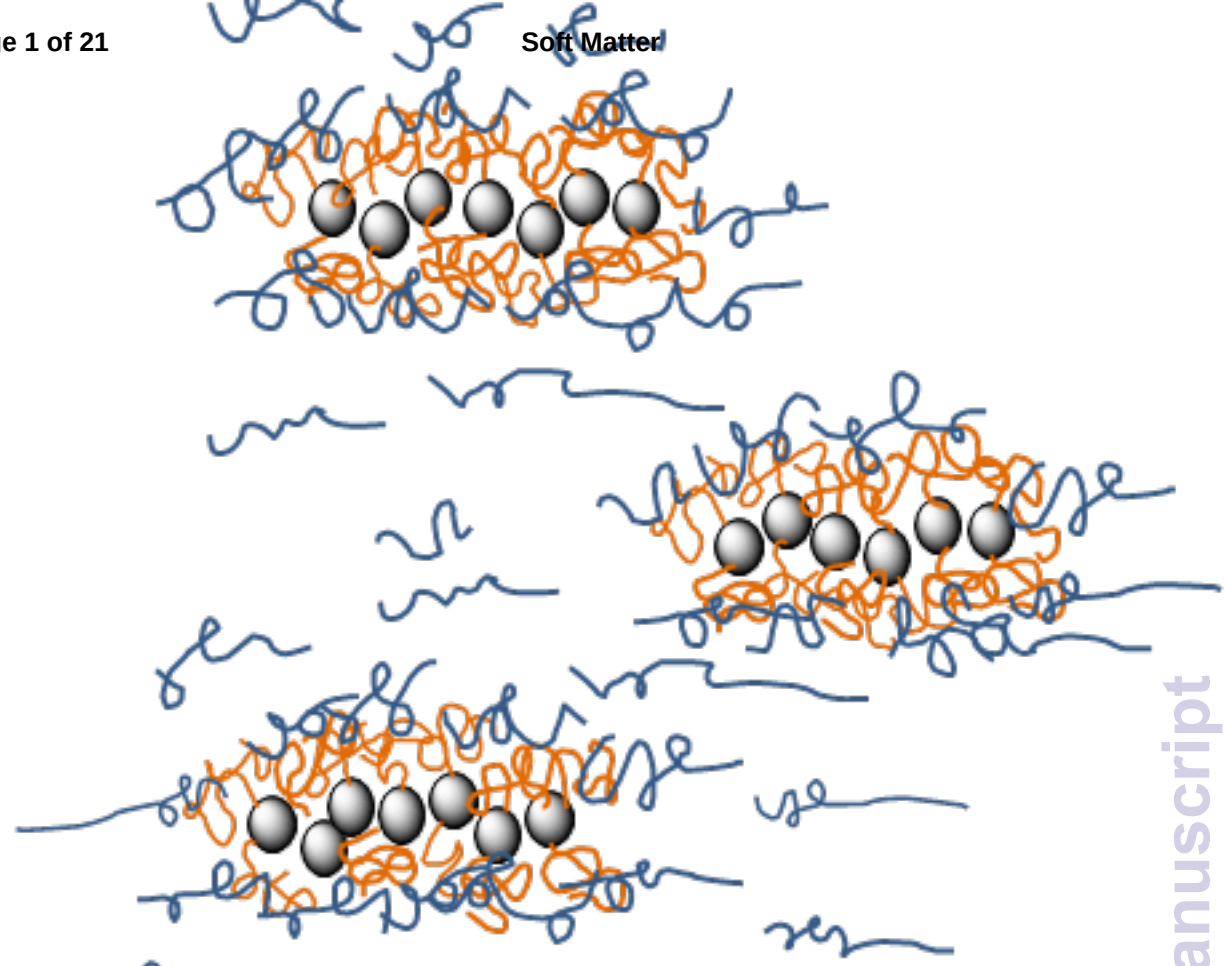

shear-induced alignment of particles

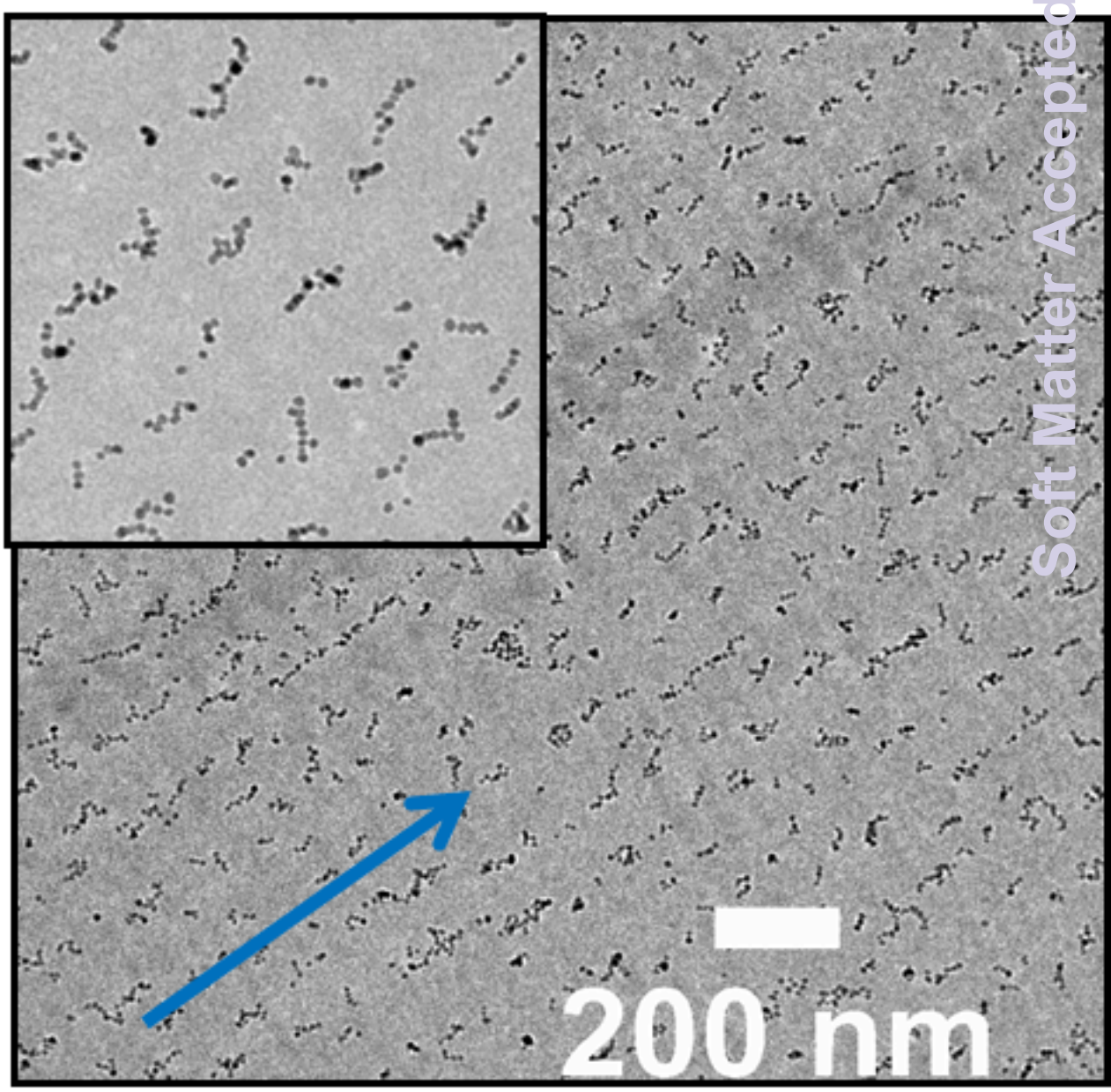

Modulating interfacial attractions of polymer-grafted nanoparticles in melts under shear

Erkan Senses, Yang Jiao and Pinar Akcora*

Department of Chemical Engineering & Materials Science, Stevens Institute of Technology

Hoboken NJ 07030 USA

*Corresponding author. pakcora@stevens.edu

ABSTRACT

Mechanical properties of polymer nanocomposites are significantly affected by spatial ordering of nanoparticles (NPs) which can be modified under shear flow fields. Polymer-grafted iron oxide NPs form strings, well-dispersed, and percolated anisotropic nanostructures depending on grafting density, and herein their mechanical properties under large oscillatory shear flows are reported. We show that flow-induced alignment of NPs is achieved with string-like structures at low particle loadings (5 wt%). Further, entropic surface tension between grafted and free chains decreases by facilitating the penetration of long matrix chains into the grafts with oscillatory shear flow. Consequently, degree of entanglements under large strain amplitudes is enhanced which is reflected in elastic properties. These results indicate that matrix polymer plays an effective role in the reinforcement of polymer-grafted NPs under large shear flow fields.

KEYWORDS: polymer-grafted nanoparticles, magnetic nanoparticles, nanocomposite, shear flow, shear-induced ordering, interface

INTRODUCTION

Ordering polymer-grafted NPs in polymer melts under shear flows holds great potential for enhancing particle dispersion and aligning anisotropic nanostructures. It is now well-established that polymer-grafted NPs self-organize into ordered morphologies of sheets, spheres and interconnected superstructures depending on grafting density, matrix and grafted chain lengths[1,2,3,4,5,6]. Effects of various morphologies on mechanical properties of polymer nanocomposites (PNCs) are commonly studied in linear viscoelastic and steady-shear experiments[4,6,7,8,9]. In our recent work, strings that are of one particle in width are created with polystyrene (PS)-grafted iron oxide NPs in bulk films[3,10]. The formation of the 1-D nanostructures is explained with the entanglements between long grafted chains and the effective dipolar interactions between particles. Further, for the same system we have reported that increasing matrix molecular weight with respect to grafted ones does not result in autophobic dewetting of grafted NPs that potentially induces attractions between particles, but rather short dispersed strings are obtained[3]. Previous works have reported that other factors such as inter-diffusion between grafted and free chains, particle size and polydispersity may be the reasons for achieving dispersed particles even in the case of grafted chains that are longer than free chains [11,12,13]. In this paper, large oscillatory shear flows are utilized to understand the consequences of inter-diffusion and matrix chain length on the mechanical behavior of composites.

External shear fields have been applied to block copolymer nanostructures to enhance their miscibility, ordering and mechanical properties in solution, melts and thin films[14,15,16]. It has been shown that diblock copolymer micelles present structural transition under flow fields between crystalline and melt states where recrystallization occurs at the critical melting shear rates[17,18]. Oscillatory shear has also been used in particle-polymer suspensions to study order-

disorder transitions[19,20,21,22]. At high particle concentrations, jamming transition is achieved with shear, and the material becomes more viscous as strain amplitude increases[23,24]. Shearing PNCs in melts will potentially influence dispersion and particularly their mechanical behavior. We focus primarily on modulating interfaces and entanglements within grafted chain-matrix under shear flow. Here, we show that mechanical properties of PS-grafted iron oxide NP nanostructures in polymer melts are enhanced and strings are aligned with oscillatory shear flows. We demonstrate that large-strain amplitudes decrease interfacial tension between hairy particles and free chains, and thus oscillatory shear flows can be an effective processing tool to order particles over large length scales.

Our system of polymer-decorated iron oxide NPs and their tunable structures in the absence of magnetic fields will find potential applications in biomaterials, sensing and separation technologies. It is difficult to align superparamagnetic NPs at nanoscale in the presence of magnetic fields at room temperature[25]. Applying shear flow fields will be an effective strategy to modulate entropic attractions between NPs with the aim of obtaining ordered structures.

MATERIALS and METHODS

Sample Preparation: PS-tethered iron oxide (Fe_3O_4) NPs were synthesized via grafting-to method as reported in our previous work[3]. 124 kg/mol and 43 kg/mol chains were grafted on nanoparticles (8nm in diameter) at different densities (0.017, 0.044 and 0.066 chains/nm^2). Particles in toluene were mixed with the host 43 kg/mol or 124 kg/mol PS matrix and sonicated for 20 s to prepare the composite solutions. Core particle concentrations of 5 and 15 wt% were used in composite preparation. Samples in solution were cast onto Teflon dishes, dried in air and then were annealed at 2 days in a vacuum oven at 150 ^{o}C.

Sample Characterization: Molecular weight of polystyrene was determined by gel permeation chromatography-light scattering (GPC/LS) using a system equipped with a VARIAN PLgel 5.0 μm Mixed–C gel column (7.5 mm ID), a multi-angle light scattering detector (miniDawn, Wyatt Technology) and a refractive index detector (Optilab rEX, Wyatt). To calculate grafting density, thermal gravimetric analysis (TGA) measurements were performed on a Q50 TGA (TA Instruments) under a constant flow of nitrogen of 20 ml/min at a heating rate of 20 °C/min, starting from room temperature up to 580 °C, and then held constant at maximum temperature for 30 min. All samples were dried in a vacuum oven at 60-80 °C prior to TGA measurement to remove moisture. Grafting density (σ) is calculated using: $\sigma = (\frac{\omega_{PS}}{100-\omega_{PS}} - \frac{\omega_0}{100-\omega_0}) \mathrm{N_A} \rho_{Fe_3O_4} / (3\pi R M_n)$, where ω_{PS} and ω_0 are the weight losses of PS-attached and bare particles, respectively, $\mathrm{N_A}$ is Avogadro constant, $\rho_{Fe_3O_4}$ is density of bulk Fe_3O_4, R is radius of a nanoparticle, and M_n is the number-average molecular weight of PS grafts.

Rheology: Measurements were performed on a strain-controlled ARES-G2 rheometer (TA Instruments) equipped with 8-mm parallel plates geometry at 150 ^{o}C under nitrogen. Samples were molded into disks with a vacuum assisted compression molder at 150 ^{o}C for 10 min and then annealed at 130 ^{o}C for 12 h. The measurements were performed after temperature equilibration time of 10 min. We monitored the sample stability in time sweep experiments during the equilibration period. Linear viscoelasticity of composites was measured by imposing oscillatory strain, $\gamma(t)=\gamma_0 sin(\omega t)$, in the linear region and frequency range between 0.1 and 100 rad/s. Large-amplitude oscillatory shear (LAOS) tests were performed at a fixed angular frequency of 1 rad/s and at various strain amplitudes from 100 to 400%, with corresponding peak shear rates of 1-4 s^{-1}. 48 strain cycles were applied for 300 s period at all strain amplitudes. Data

were collected at a sampling frequency of 300 Hz, giving 1885 points per cycle and last 7 cycles were analyzed where the quasi-steady-state stresses were reached. The samples were cooled below T_g (~105 ^oC) in ~15 s with normal force controlled within +/- 1N to avoid thermal strain. Small pieces were cut from quenched samples for TEM investigation after deformation. Since the sample amount is lower in the end of 400% strain measurements, only the elastic and viscous moduli obtained from measurements at 100% strain amplitude are presented throughout this paper (see Table S1 in Supporting Information).

Structural analysis: Samples were microtomed from their bulk films with a diamond knife at room temperature and analyzed in transmission electron microscopy (FEI CM20 FE S/TEM) at 200 keV. Sections were microtomed parallel to the applied shear direction in all samples.

Spatial distribution function: Particles were located in TEM images using a MATLAB based particle tracking tool (Figure S1). The x-y coordinates of particles were then used to calculate radial distribution functions. The isotropic *g(r)*'s at distance *r* were obtained by normalizing the number of particles located within a differential area $g(r)=N(r)/(\sigma 2\pi r dr)$, where σ is the average number density of particles in TEM area. The angular $g(r, \alpha)$'s were determined by counting the number particles within a differential area $(2rd\alpha dr)$ in directions of $\pi/4$ and $3\pi/4$ within $d\theta$: 14^0.

RESULTS and DISCUSSION

Our previous work has shown that at low grafting densities, iron oxide NPs with short grafts (43 kg/mol) form aggregated anisotropic clusters; and the longer grafts (124 kg/mol) form strings[3]. While structural transitions from elongated branched chains to spheres, and to short chains were observed by increasing the graft density of short grafted chain lengths; strings and isolated structures were reported for the long grafts (Figure 1). TEM micrographs of the samples[3] used in

this work are shown in Figure S2. Here, we present the mechanical behavior and dispersion of these composites (see also Table S1 for sample specifications) to examine inter-particle attractions under large shear flow fields.

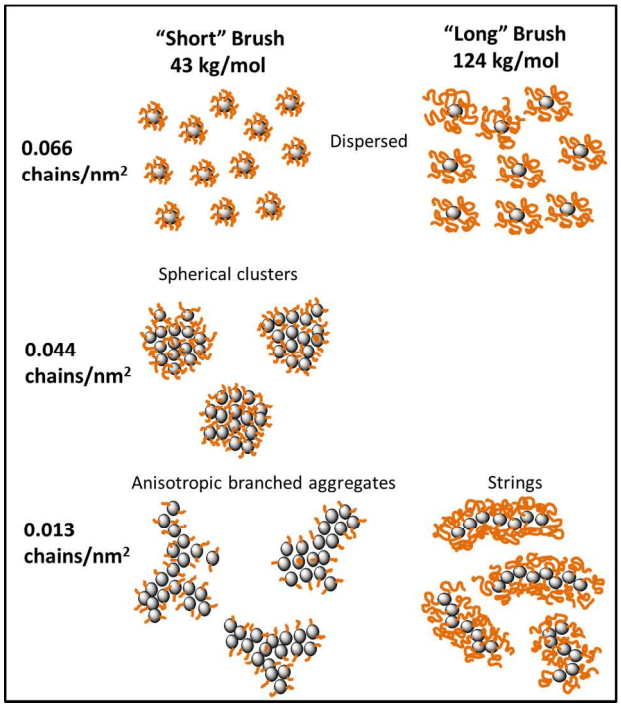

Figure 1. Schematic representation of morphologies observed for polystyrene-grafted iron oxide nanoparticles with two graft lengths: 43 and 124 kg/mol at different grafting densities. TEMs of all the structures are shown in Figure S2.

Linear rheology measurements: Prior to applying large shear to the existing structures in our composites, we present their linear viscoelastic behavior, providing the relaxation behavior of structures in equilibrium. Figure 2a shows elastic and viscous moduli of 43 kg/mol polymer grafted particles at different grafting densities dispersed in 124 kg/mol PS matrix. The composite with dispersed particles at 0.066 chains/nm^2 density presents slightly lower modulus than other composites with aggregated morphologies. On the other hand, in the case of a longer grafted

chain length (124 kg/mol), strings in which fillers are directly connected at low fraction (5 wt%) have lower modulus than dispersed particles (Figure 2b). While higher elastic modulus is typically associated to the connectivity of particles, the non-interacting grafted particles behave more elastic. The conflicting results on these two systems with short and long graft lengths indicate that viscoelastic properties are not sensitive to nanostructural differences within composites. This is also supported with the identical linear data of matrix homopolymer and its composite containing aggregated anisotropic clusters (Figure 3a). Moreover, strings exhibit lower elastic modulus than clustered particles of short grafts (43 kg/mol), which can be explained with the larger energy required to break the large clusters within branched aggregates. In summary, dispersion states cannot simply explain nano-reinforcement in linear mode, and nonlinear rheology experiments are essential to understand the role of interfacial entanglements on reinforcement effect as chains can disentangle, align and stretch when particle structures coarsen and break during large shear. To observe the effect of connectivity of strings on linear results, we have prepared 15 wt% composites in addition to 5 wt%. Figure 3b shows that cross-over modulus shifted to a lower frequency in 15 wt% sample, indicating slower relaxations due to percolation of strings.

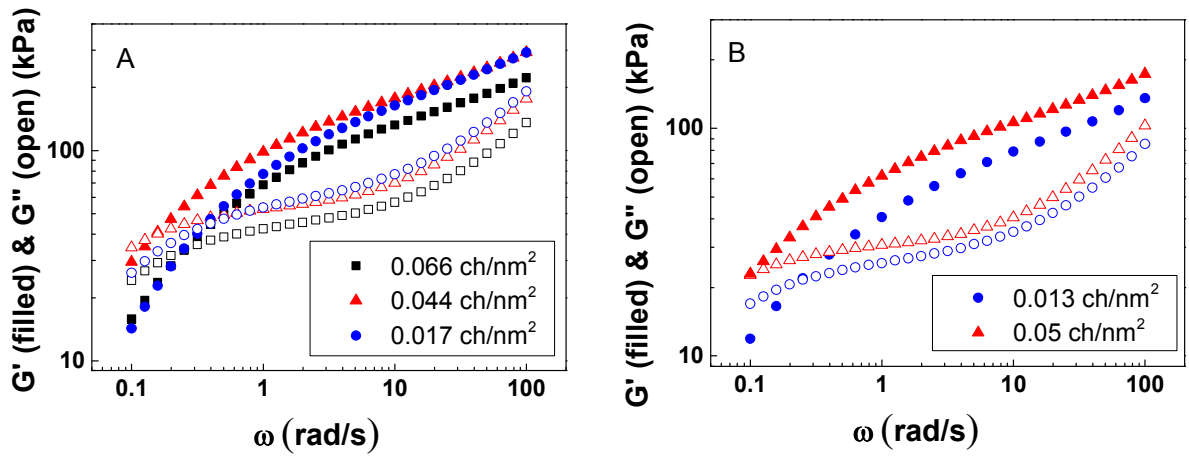

Figure 2. Effect of grafting density (in chains/nm^2) on linear viscoelastic data of **(a)** 43 kg/mol and **(b)** 124 kg/mol grafted-PS in 124 kg/mol PS matrix. Measurements are conducted at 150 ^{o}C, 1 rad/s and 10% strain amplitude. Particle loading is 5 wt%.

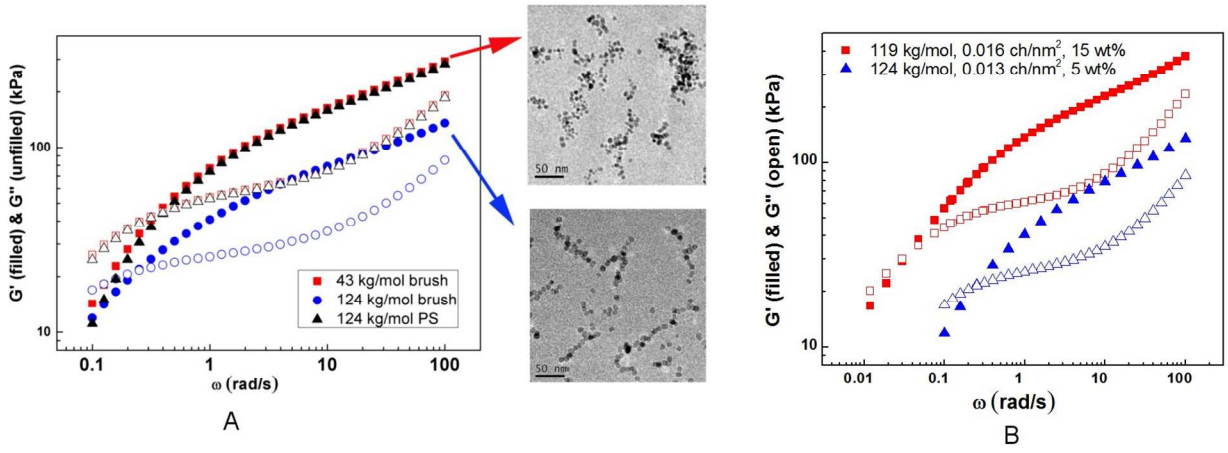

Figure 3. (a) Viscoelastic data of PS homopolymer (124 kg/mol) and its composites prepared with grafted NPs of varying graft lengths (43 kg/mol PS-grafted NPs with 0.017 chains/nm^2 density, and 124 kg/mol grafted NPs at 0.013 chains/nm^2 density) and corresponding TEM micrographs. **(b)** Effect of particle loading on the viscoelastic properties of a string forming

composite. Grafted polymer is 119 and 124 kg/mol PS with 0.016 and 0.013 chains/nm^2 on iron oxide nanoparticles, respectively.

In our previous work on non-attractive PS-SiO_2 composite system, we have reported that at large strains polymer deforms similar to polymer networks due to possible stretching of chains between particle clusters and breaking of interconnected particles manifests yielding at intermediate strains[26]. On the contrary, in attractive PMMA-SiO_2 composite where particles are well-dispersed, stress increases monotonically with strain and presents no yielding[27]. The self-stiffening behavior observed after multiple deformation stages suggests that stretching and deformation of polymer chains were different in PMMA composite, and entanglement of chains near particle surfaces can be tuned with oscillatory shear deformations. These recent reported results[26,27,28] on "bare" particle filled polymers guide us to investigate interface effects between grafted and matrix chains in LAOS since it is expected that shear flow fields alter the interpenetration between grafts and free chains.

Nonlinear Results on Composites: We present the nonlinear behavior of PS homopolymer and its disentanglement above 200% strain amplitude in Figure S3. Figure 4a shows the unusual elastic behavior of our composite consisting of "short" (43 kg/mol) PS-grafted NPs in 124 kg/mol matrix at 100% strain. It is shown that elastic modulus increases with increasing grafting density. Contrary to this, elastic modulus decreases with grafting density for the same particles in 43 kg/mol matrix (Figure 4b).

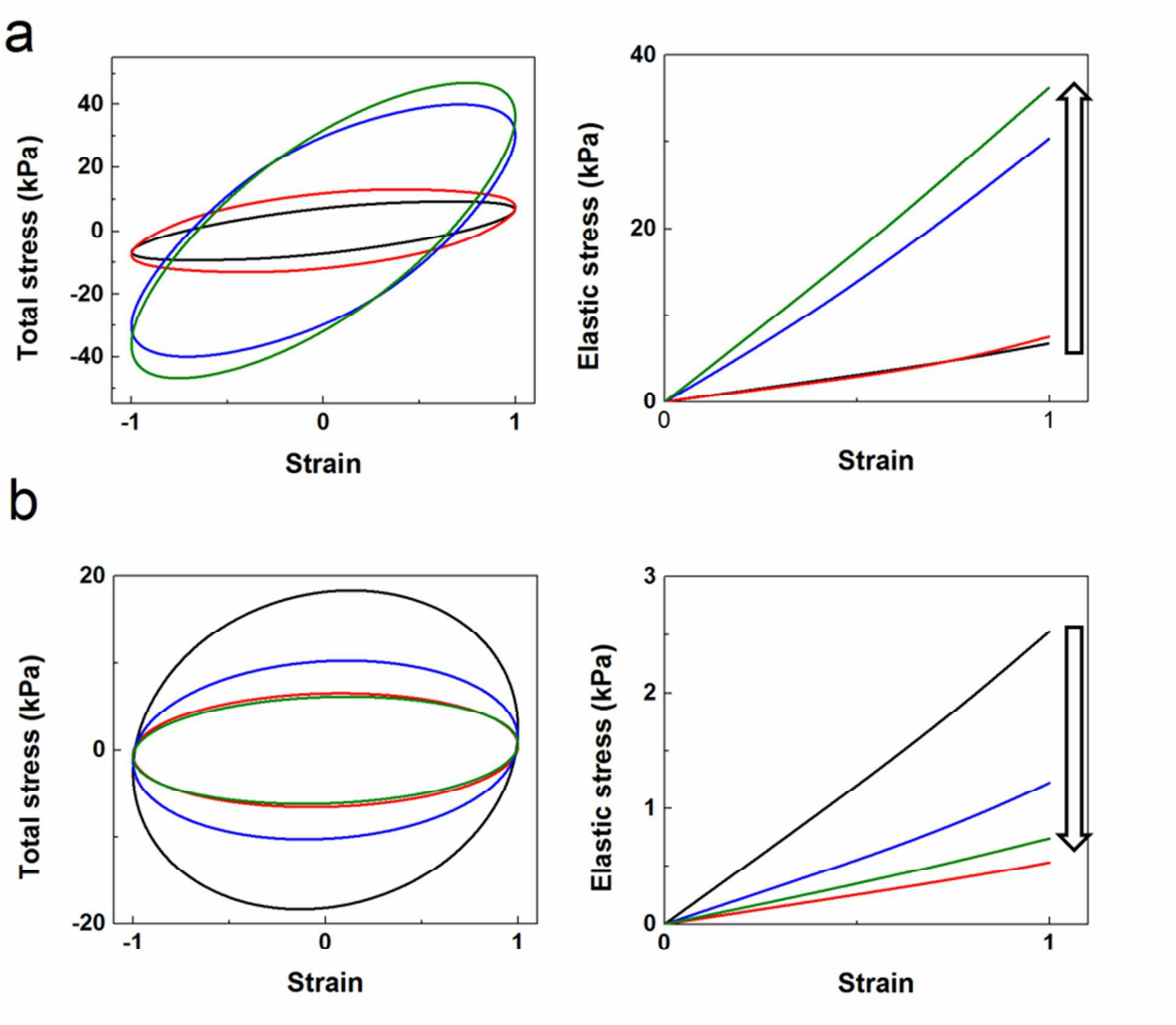

Figure 4. (a) Lissajous curves obtained at ω=1 rad/s and γ_0=100% and corresponding elastic stress-strain curves for PS (43 kg/mol)-grafted iron oxide NPs with different grafting densities (σ), shown in different colors (black: homopolymer; red: 0.017 chains/nm^2; blue: 0.044 chains/nm^2; green: 0.066 chains/nm^2). NPs are in **(a)** 124 kg/mol and **(b)** 43 kg/mol matrices.

Figure 5 summarizes the elastic response at 100% strain in two matrices as a function of grafting density. The effect of interface attractions are clearly seen in 124 kg/mol matrix, and that elastic modulus increases with grafting density due to shear-induced entanglements of grafts with long

matrix polymer under large oscillatory shear flows. It is important to note that particle dispersion did not change with deformation for 0.066 chains/nm^2 graft density, and the spherical clusters of ~100 nm in size were observed for other densities which seem to be consistent with their undeformed states (see Supporting Information Figure S4 for TEMs on deformed 43 kg/mol PS-grafted NPs composites at different graft densities in 124 kg/mol matrix). Conversely, the same particles present softening with increasing densities when dispersed in 43 kg/mol matrix. We also note that 43 kg/mol matrix chains that are less likely to stretch under shear flows presumably cannot play an effective bridging role between the grafted chains.

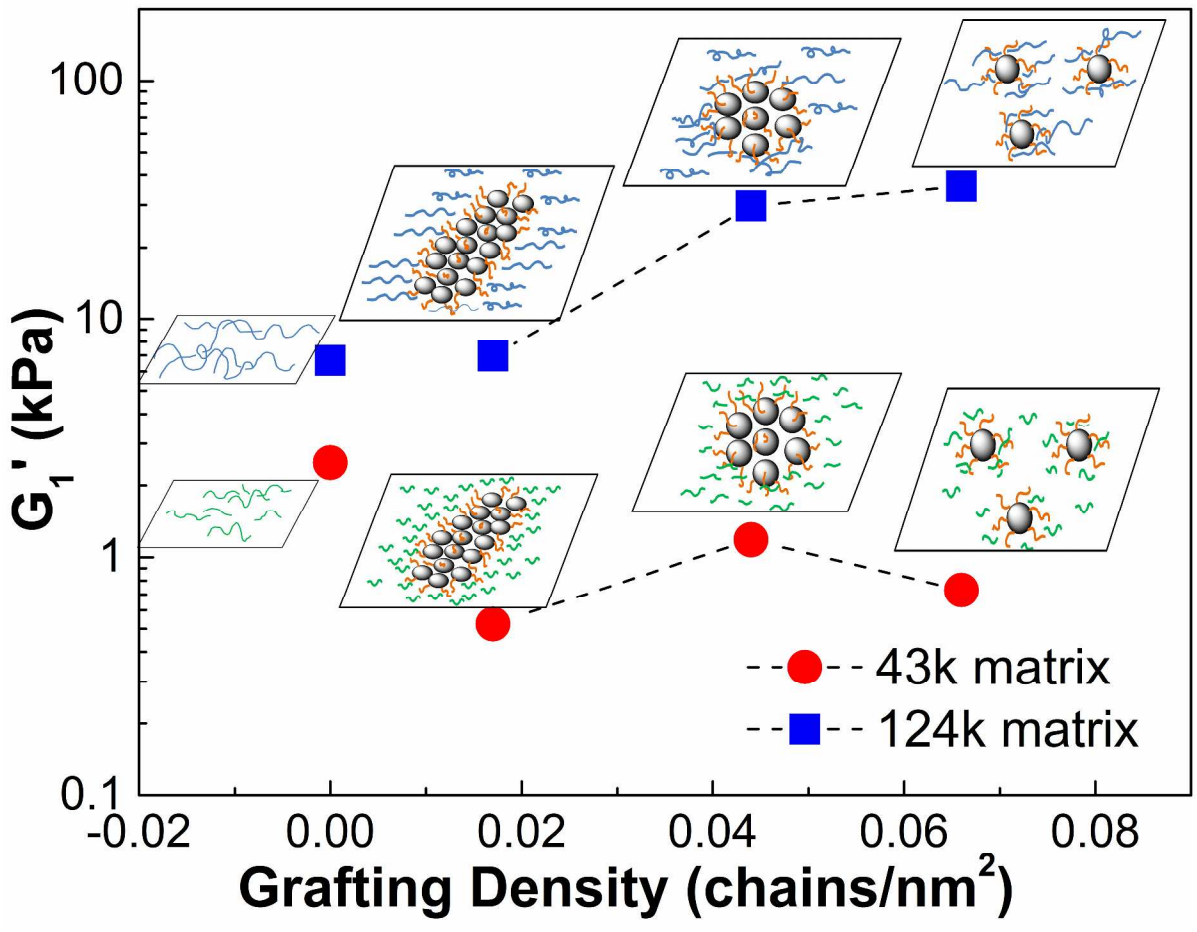

Figure 5. Elastic moduli of PS (43 kg/mol)-grafted iron oxide NPs dispersed in two PS matrices (43 and 124 kg/mol) at different grafting densities. Data is collected at 100% strain amplitude at

150 ^{o}C. Elastic moduli of PS homopolymers - 124 kg/mol (blue), 43 kg/mol (red) - are marked as single points. Composites contain 5 wt% particles. Cartoons represent the state of particle structures and their interactions with the short and long free chains as oscillatory shear is applied.

Effect of matrix chain penetrations into the "long" PS-grafted NPs under shear is displayed in Figure 6 by the reinforcement factor (elastic modulus of composite normalized with its matrix modulus) versus the ratio of grafted to matrix molecular weights. Large reinforcement factor obtained in 124 kg/mol matrix is, -similarly-, associated with interfaces getting stronger under shear. We observe this nonlinear reinforcement clearly in the raw stress data which show that composite of 124 kg/mol PS-grafted NPs does not soften in its matrix as homopolymer does under many oscillations (Figure S5**)** and 43 kg/mol PS-grafted NPs soften similar to its matrix but reaches steady state quickly since it contains less entanglements. The elastic and reinforced behavior of composites prepared with the two grafted NP systems, presented in Figures 5 and 6, substantiate that the self-reinforcement depends on mixing of grafted chains with matrix polymer under large oscillatory shears.

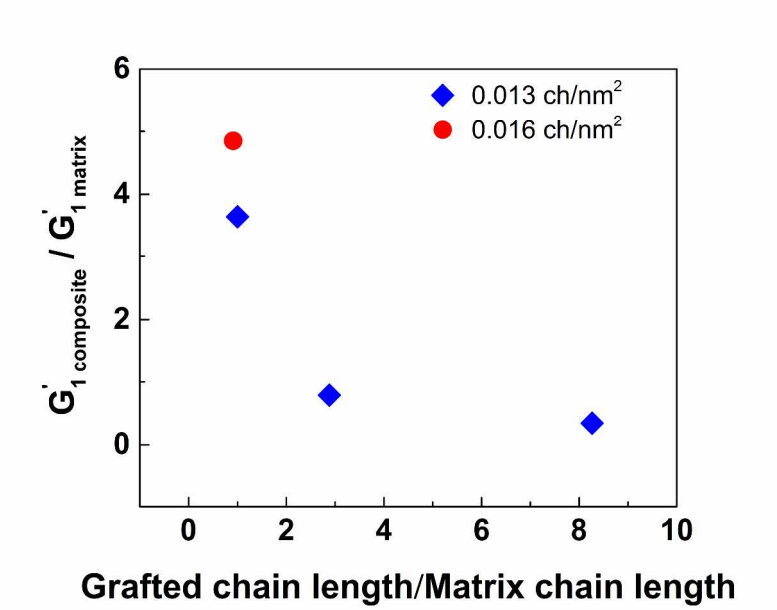

Figure 6. Normalized elastic moduli of PS (124 kg/mol) grafted NPs with 0.013 chains/nm^2 density, dispersed in varying matrix molecular weights, measured at 150 ^{o}C, 100% strain amplitude and 1 rad/s. The red data point is the 119 kg/mol grafted NPs dispersed in 130 kg/mol PS with 0.016 chains/nm^2 at 15 wt% loading.

Alignment of Polymer-Grafted Nanoparticles with Shear Flow: In a typical steady-shear test, a constant shear rate is applied and strain increases linearly with time. Such experiment can result in disentanglement, orientation and stretching of a polymer chain depending on the ratio of shear rate to Rouse time. Moreover, particle clusters experience large displacements in unidirectional large strains which may cause coalescence of microstructures[8]. On the other hand, deformation of a sample in LAOS involves relaxation and stretching of chains in many cycles of oscillation between linear and nonlinear regimes as represented in Figure S6. More importantly, as the sample is repeatedly strained in forward and backward direction, the average displacement of the particles is nearly zero; meaning the uniformly distributed strings are less likely to

aggregate, but they can orient in the shear flow fields. We chose LAOS as it allows both modulating the grafted chain-matrix entanglements and aligning nano-strings.

For this purpose, we deformed the string forming NPs at increasing strain amplitudes as schematically shown in Figure 7a. Each deformation step consists of 300 s deformation followed by quenching below the glass-transition temperature in order to freeze the structure formed during LAOS. Randomly dispersed strings at 100% strain amplitude and their alignment at 300 and 400% amplitudes are presented in Figure 7b. We quantified the orientation of strings by analyzing the pair distribution functions of particles along two orientations 45^0 and 135^0 as a function of radial distance r normalized by the particle radius (R_0). Figure 7c shows that depth of minimum decreases by increasing strain from 100 to 400% since more particles join the anisotropy during alignment, indicating that strings are aligned at 45^0 with 400% strain amplitude. It was observed that after annealing the aligned sample for 3 days at 150 ^oC, chains returned to their disordered string arrangements as shown in Figure 8c, which reveals the orientations are facilitated with grafted chains and this process can be reversed upon annealing. When strain amplitude is further increased to 500%, strings loose their orientation and break down into shorter disordered chains (Figure 8b). In the case of 15 wt% particle loading, however, the string nature of particles prevails but the particles do not flow align (Figure S7). This may be due to reformation of crowded strings in a composite network under applied shear.

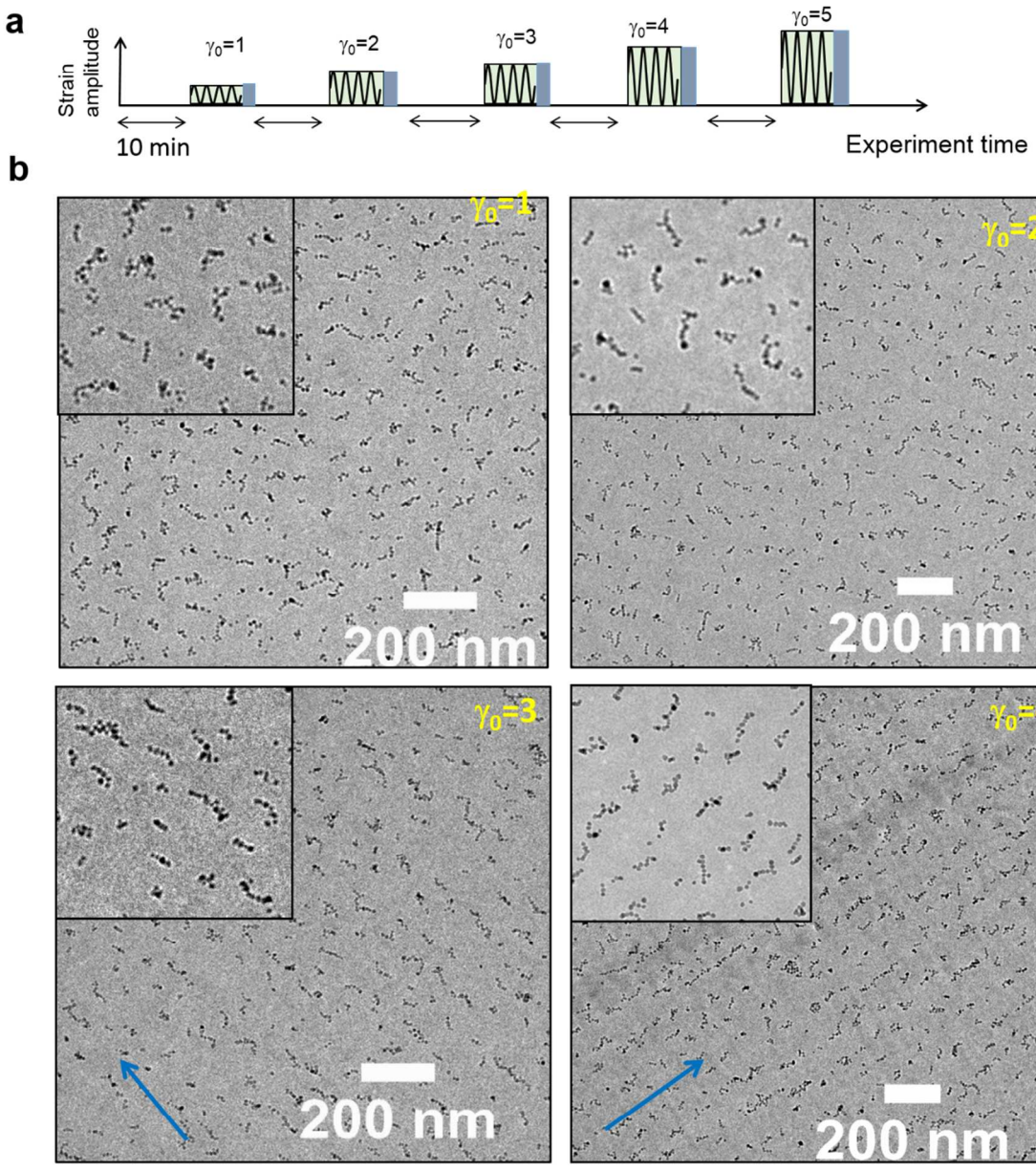

Figure 7. (a) Large strain amplitude deformation and sampling sequence diagram. Blue regions are times for quenching to room temperature and sampling for imaging. **(b)** TEM micrographs of PS (124 kg/mol)-grafted iron oxide NPs in 124 kg/mol PS matrix after deformations at varying strains (γ: 1-4) at 1 rad/s. Insets display the enlarged sections from TEMs. **(c)** Isotropic pair distribution functions, $g(r)$, of the composite and angular dependent pair distribution functions, $g(r,\alpha)$, at 100% and 400% strain amplitudes at 45° and 135° angles.

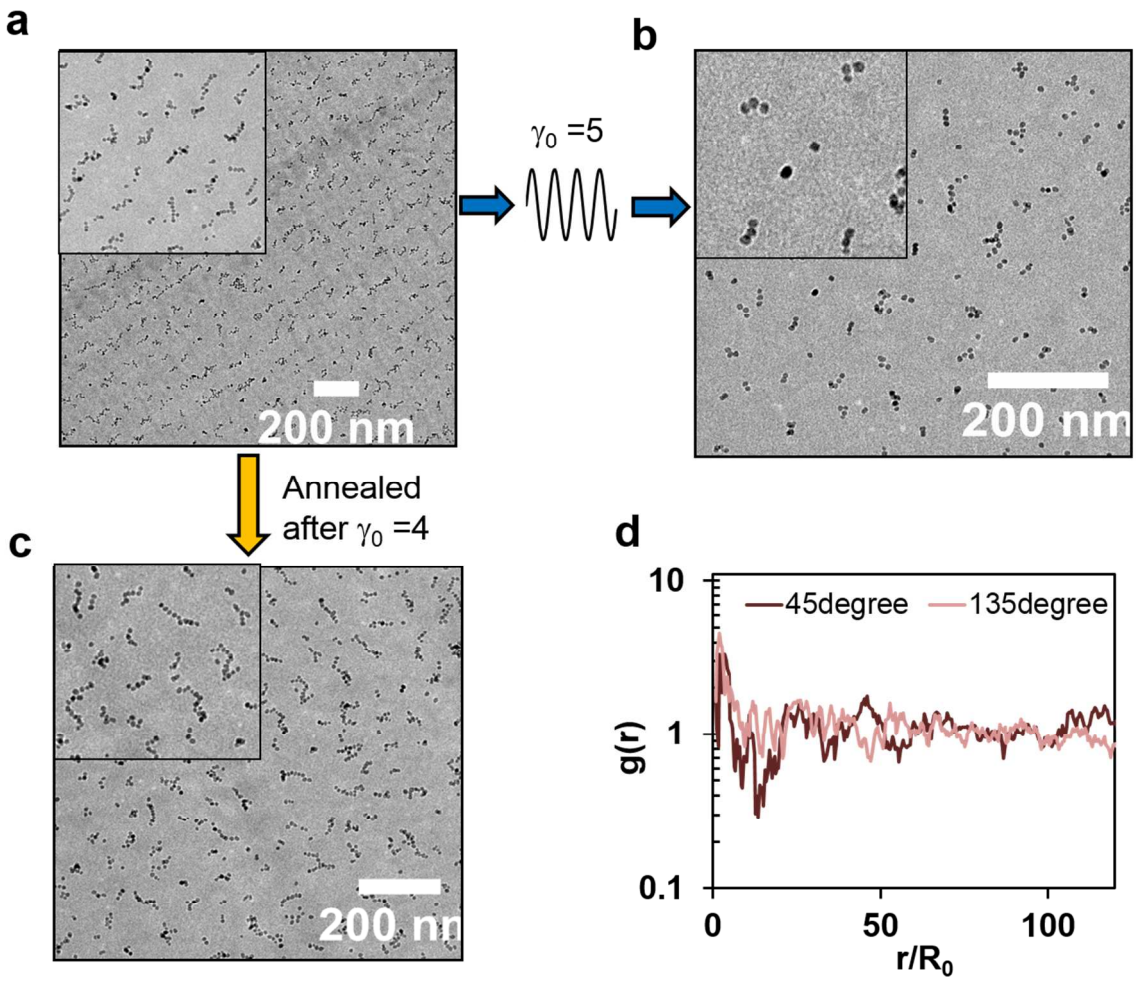

Figure 8. (a-b) Aligned strings at 400% strain are broken into small strings when the strain amplitude is further increased to 500%. **(c)** The same aligned strings are disoriented when the sample is annealed at 150 ^{o}C for 3 days and **(d)** corresponding *g(r, α)*'s in 45^0 and 135^0 angles.

In summary, we show that strings of hairy NPs are aligned at low particle loadings under large amplitude oscillatory shear due to enhanced matrix-graft entanglements, contrary to the results reported on structural coarsening of NPs under flow rather than aligning them[8]. We also suggest that interfacial strengthening of grafts with free chains may help alignment of spherical NPs under shear flows. While elastic moduli values are presented for 100% strain amplitude in Figures 4-6, we conjecture that elastic properties may improve at higher strains, as denoted by preserved structures.

CONCLUSIONS

We show that nonlinear oscillatory experiments are sensitive to dispersion of grafted particles unlike their linear data, and provide valuable mechanical information on the role of grafted chain-matrix interactions as grafting density and matrix chain lengths are varied. Enhanced elastic property is attributed to the shear-induced entanglement of long matrix with the grafted chains under oscillatory shear flows. We suggest that interfacial strengthening helps in orienting the string-like structures in one direction and forms long-range alignment at 300-400% strain amplitudes. Reinforcement factor for string structures decreases with matrix molecular weights as the short free chains cannot form "permanent" entanglements with the grafts. In the same vein, the shorter grafted chains behave stiffer when mixed with free chains longer than the grafted ones due to the shear-flow driven miscibility of particles. In conclusion, effective bridging of soft (polymer-grafted) particles through the interpenetration of long matrix chains under shear allows modulating the interfacial attractions. Consequently, stiffened interfaces

between matrix and grafted chains can be achieved under large oscillatory shear deformations and ordered strings are formed, which can be reversed upon annealing.

Supporting Information. TEM micrographs of 43 and 124 kg/mol PS grafted particles at various graft densities; raw stress-time data for homopolymers and composites; TEM micrographs of deformed composites from 43 kg/mol PS-grafted NPs; schematic representation of chains deforming under large amplitude oscillatory deformation; a representation of locating particles in a TEM micrograph; Table for sample characteristics with their loss and storage moduli values.

ACKNOWLEDGEMENTS

We gratefully acknowledge financial support from the Stevens start-up funds and NSF-CAREER (Award # 1048865) from DMR.

REFERENCES

1 Akcora, P. *et al.* Anisotropic self-assembly of spherical polymer-grafted nanoparticles. *Nature Materials* **8**, 354-359 (2009).
2 Moll, J. F. *et al.* Mechanical reinforcement in polymer melts filled with polymer grafted nanoparticles. *Macromolecules* **44**, 7473-7477 (2011).
3 Jiao, Y. & Akcora, P. Assembly of polymer-grafted magnetic nanoparticles in polymer melts. *Macromolecules* **45**, 3463-3470 (2012).
4 McEwan, M. & Green, D. Rheological impacts of particle softness on wetted polymer-grafted silica nanoparticles in polymer melts. *Soft Matter* **5**, 1705-1716 (2009).
5 Kumar, S. K., Jouault, N., Benicewicz, B. & Neely, T. Nanocomposites with polymer grafted nanoparticles. *Macromolecules* **46**, 3199-3214 (2013).
6 Chevigny, C., Jouault, N., Dalmas, F., Boué, F. & Jestin, J. Tuning the mechanical properties in model nanocomposites: Influence of the polymer-filler interfacial interactions. *Journal of Polymer Science, Part B: Polymer Physics* **49**, 781-791 (2011).
7 Kim, D., Srivastava, S., Narayanan, S. & Archer, L. A. Polymer nanocomposites: Polymer and particle dynamics. *Soft Matter* **8**, 10813-10818 (2012).
8 Moll, J. *et al.* Dispersing grafted nanoparticle assemblies into polymer melts through flow fields. *ACS Macro Letters* **2**, 1051-1055 (2013).

9 Pryamitsyn, V. & Ganesan, V. Mechanisms of steady-shear rheology in polymer-nanoparticle composites. *Journal of Rheology* **50**, 655-683 (2006).

10 Jiao, Y. & Akcora, P. Effect of Ionic Groups on the Polymer-Grafted Magnetic Nanoparticle Assemblies. *Macromolecules*, doi: 10.1021/ma402509b (2014).

11 Corbierre, M. K., Cameron, N. S., Sutton, M., Laaziri, K. & Lennox, R. B. Gold nanoparticle/polymer nanocomposites: Dispersion of nanoparticles as a function of capping agent molecular weight and grafting s. *Langmuir* **21**, 6063-6072 (2005).

12 Green, P. F. The structure of chain end-grafted nanoparticle/homopolymer nanocomposites. *Soft Matter* **7**, 7914-7926 (2011).

13 Martin, T. B., Dodd, P. M. & Jayaraman, A. Polydispersity for tuning the potential of mean force between polymer grafted nanoparticles in a polymer matrix. *Physical Review Letters* **110** (2013).

14 Hamley, I. W. Structure and flow behaviour of block copolymers. *Journal of Physics Condensed Matter* **13**, R643-R671 (2001).

15 Laurer, J. H., Pinheiro, B. S., Polis, D. L. & Winey, K. I. Persistence of surface-induced alignment in block copolymers upon large-amplitude oscillatory shear processing. *Macromolecules* **32**, 4999-5003 (1999).

16 Hong, Y. R., Adamson, D. H., Chaikin, P. M. & Register, R. A. Shear-induced sphere-to-cylinder transition in diblock copolymer thin films. *Soft Matter* **5**, 1687-1691 (2009).

17 López-Barrón, C. R., Porcar, L., Eberle, A. P. R. & Wagner, N. J. Dynamics of melting and recrystallization in a polymeric micellar crystal subjected to large amplitude oscillatory shear flow. *Physical Review Letters* **108** (2012).

18 Stellbrink, J., Lonetti, B., Rother, G., Willner, L. & Richter, D. Shear induced structures of soft colloids: Rheo-SANS experiments on kinetically frozen PEP-PEO diblock copolymer micelles. *Journal of Physics Condensed Matter* **20** (2008).

19 Pasquino, R., Snijkers, F., Grizzuti, N. & Vermant, J. The effect of particle size and migration on the formation of flow-induced structures in viscoelastic suspensions. *Rheologica Acta* **49**, 993-1001 (2010).

20 Pham, K. N. *et al.* Yielding behavior of repulsion- and attraction-dominated colloidal glasses. *Journal of Rheology* **52**, 649-676 (2008).

21 Chen, L. B. *et al.* Structural changes and orientaional order in a sheared colloidal suspension. *Physical Review Letters* **69**, 688-691 (1992).

22 Chen, L. B., Ackerson, B. J. & Zukoski, C. F. Rheological consequences of microstructural transitions in colloidal crystals. *Journal of Rheology* **38**, 193-216 (1994).

23 Srivastava, S., Shin, J. H. & Archer, L. A. Structure and rheology of nanoparticle-polymer suspensions. *Soft Matter* **8**, 4097-4108 (2012).

24 Srivastava, S., Archer, L. A. & Narayanan, S. Structure and transport anomalies in soft colloids. *Physical Review Letters* **110** (2013).

25 Lalatonne, Y., Richardi, J. & Pileni, M. P. Van der Waals versus dipolar forces controlling mesoscopic organizations of magnetic nanocrystals. *Nature Materials* **3**, 121-125 (2004).

26 Senses, E. & Akcora, P. Mechanistic model for deformation of polymer nanocomposite melts under large amplitude shear. *Journal of Polymer Science, Part B: Polymer Physics* **51**, 764-771 (2013).

27 Senses, E. & Akcora, P. An interface-driven stiffening mechanism in polymer nanocomposites. *Macromolecules* **46**, 1868-1874 (2013).

28 Papon, A. *et al.* Unique nonlinear behavior of nano-filled elastomers: From the onset of strain softening to large amplitude shear deformations. *Macromolecules* **45**, 2891-2904 (2012).